CHAPTER V

RESULTS AND DISCUSSION

5.1 Computer-simulated results of ideal cases of pigment dispersion

In this work, the Monte-Carlo Technique was used to create random patterns for two ideal cases of pigment dispersion. A computer code was written in the QBASIC language (see in Appendix A3). It used mathematical functions to generate pseudo-uniform random numbers and pseudo-normal random numbers which are used to create two different ideal types of dispersion patterns. The objectives of this computer experiment were to evaluate and compare pigment dispersion states in terms of the fractal dimension calculated either from the quantity given by equation (3.4) or by Terashita's method, and to elucidate the relationship between the sample population size and the observed values of the fractal dimension.

5.1.1 Random pattern of pigment dispersion

1) Uniform random dispersion

Figure 5.1 shows an example of the uniform random dispersion with sample population size equal to 100.

2) Normal random dispersion

In this case an example of the normal (Guassian) random dispersion with sample population size equal to 100 is shown in Figure 5.2. In this figure, it can be seen that the pigment particles were randomly dispersed around the center of a sample in the fashion of a two-dimensional normal distribution.

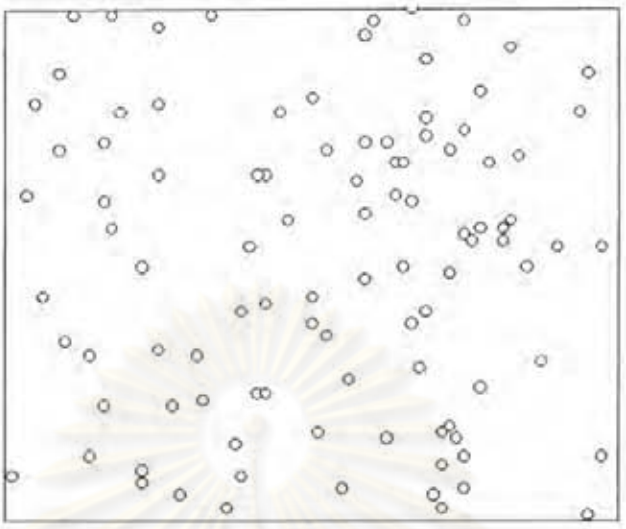

Figure 5.1 Example of uniform random dispersion of pigment particle obtained from computer simulation

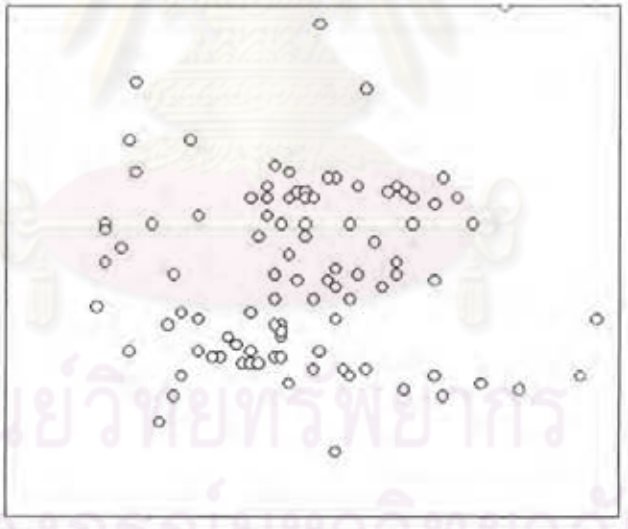

Figure 5.2 Example of normal random dispersion of pigment particles obtained from computer simulation

5.1.2 Effect of sample population size on the fractal dimension

To quantify the dispersion of pigment particles in plastic, a novel type of indices called the fractal dimension, D, was used to quantify the degree of dispersion in the sample. The fractal dimension may be evaluated by either

counting the number, N(r), of subsections that contain at least one pigment particle (Eq. 3.4) or by calculating the coefficient of variation, Ds, (Terashita's approach). In this section, the relationship between the sample population size and the observed fractal dimension is discussed as follows.

1) Fractal dimension from Eq. 3.4

The relationship between the sample population size and the fractal dimension was listed in Table 5.1 and shown in Figure 5.3.

Table 5.1 Computer-simulated results (Fractal dimension is found using equation (3.4) for the region of large n)

Sample population size	Fractal dimension (D)	
	Uniform random dispersion	Normal random dispersion
10	0.0597	0.0675
64	0.1328	0.2568
256	0.4453	0.6843
640	0.8287	0.9602
1280	1.1623	1.1935
3200	1.5778	1.4327
6400	1.8046	1.5797
12800	1.946	1.7032

From the results of Figure 5.3, it can be seen that the observed fractal dimension (D), for both the uniform and normal dispersion, increased rapidly when the sample population size first increased. As the sample population size further increased, the fractal dimension increased more gradually. Thus theoretically, the

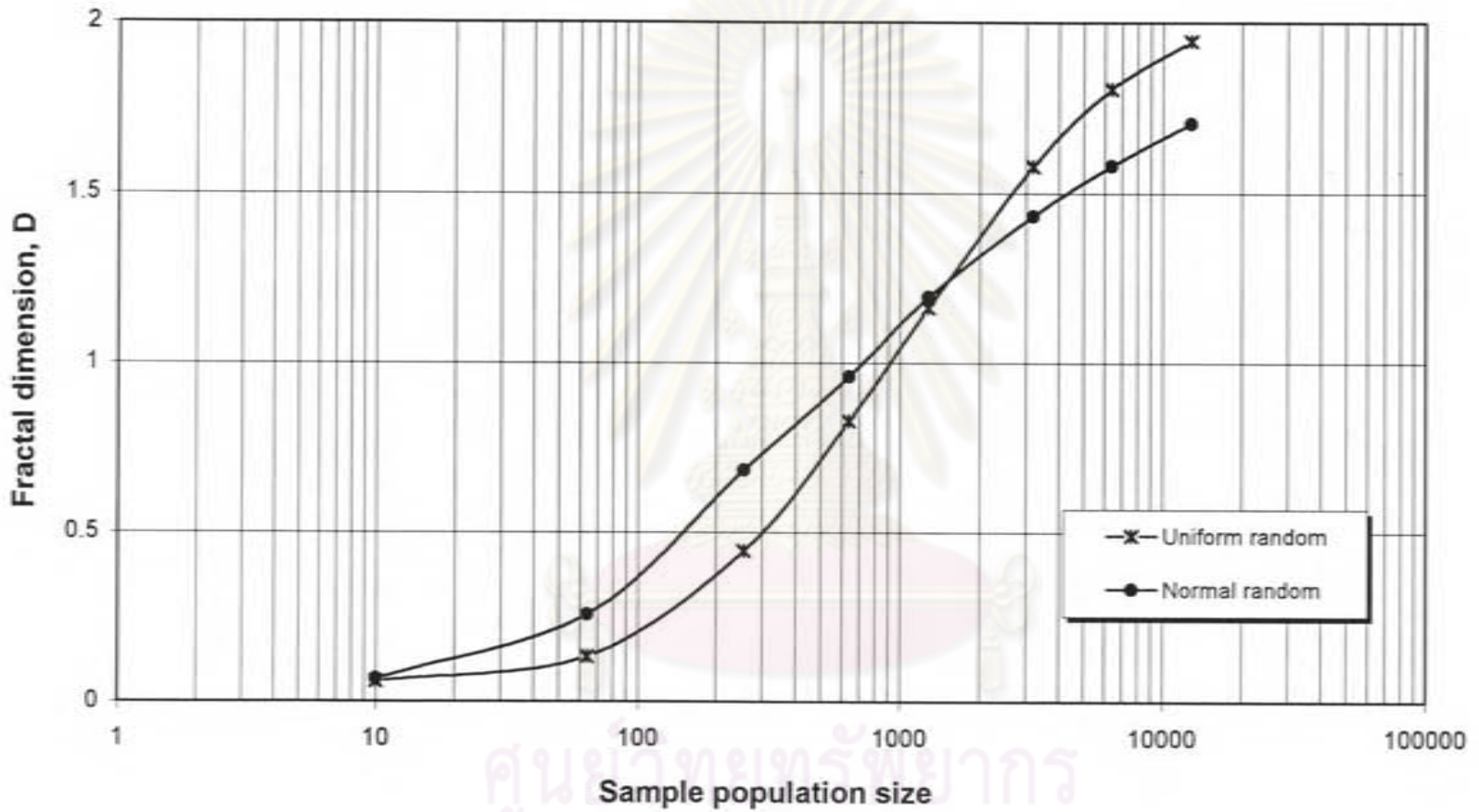

Figure 5.3 Relationship between the observed fractal dimension and the sample population size in the present study

fractal dimension for the uniform random dispersion (homogeneous mixture) ranged from nearly zero to almost 2, whereas the fractal dimension for the normal random dispersion ranged from about 0.07 to 1.70. An apparent contradiction was that the observed fractal dimension for the normal random dispersion was somewhat greater than that for the uniform random dispersion when the sample population size was smaller than 1200. Above 1200 the observed fractal dimension for the uniform random dispersion was, as expected, greater than that for the normal random dispersion. At the sample population size around 1200, the fractal dimensions for both cases were about 1.25. In addition, both types of dispersion gave relatively small difference in the fractal dimension.

The actual reason for the apparent contradiction is that even when the sample population size was much smaller than the number of the finely divided subsections, the fractal dimension was always determined from the slope in the region of large n.

As shown in Figure 5.3, at a sample population size smaller than 1200 the observed fractal dimension for the normal random dispersion was greater than for the uniform random dispersion. It apparently contradicts the fractal concept used to evaluate the dispersibility of pigment in this work where the fractal dimension should increase as the dispersion becomes more uniform. Therefore, in the following section the same fractal dimension was recalculated from the slope in the appropriate region of n, which provided the maximum slope. The results of the recalculation were shown in Table 5.2 and Figure 5.4.

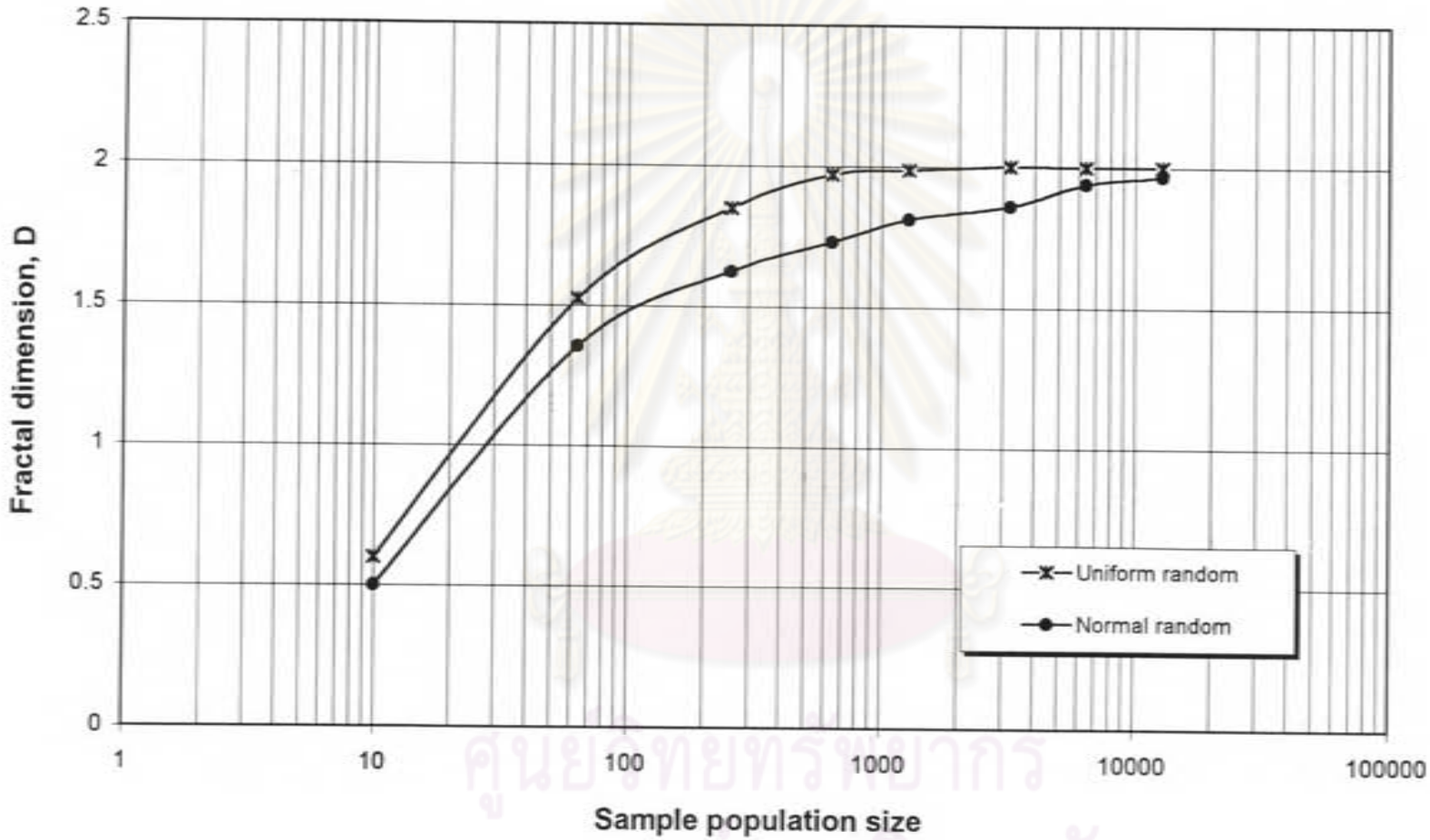

Figure 5.4 Relationship between the observed fractal dimension and the sample population size in the present study (using Eq. (3.4)) for the region of n which provided the maximum slope

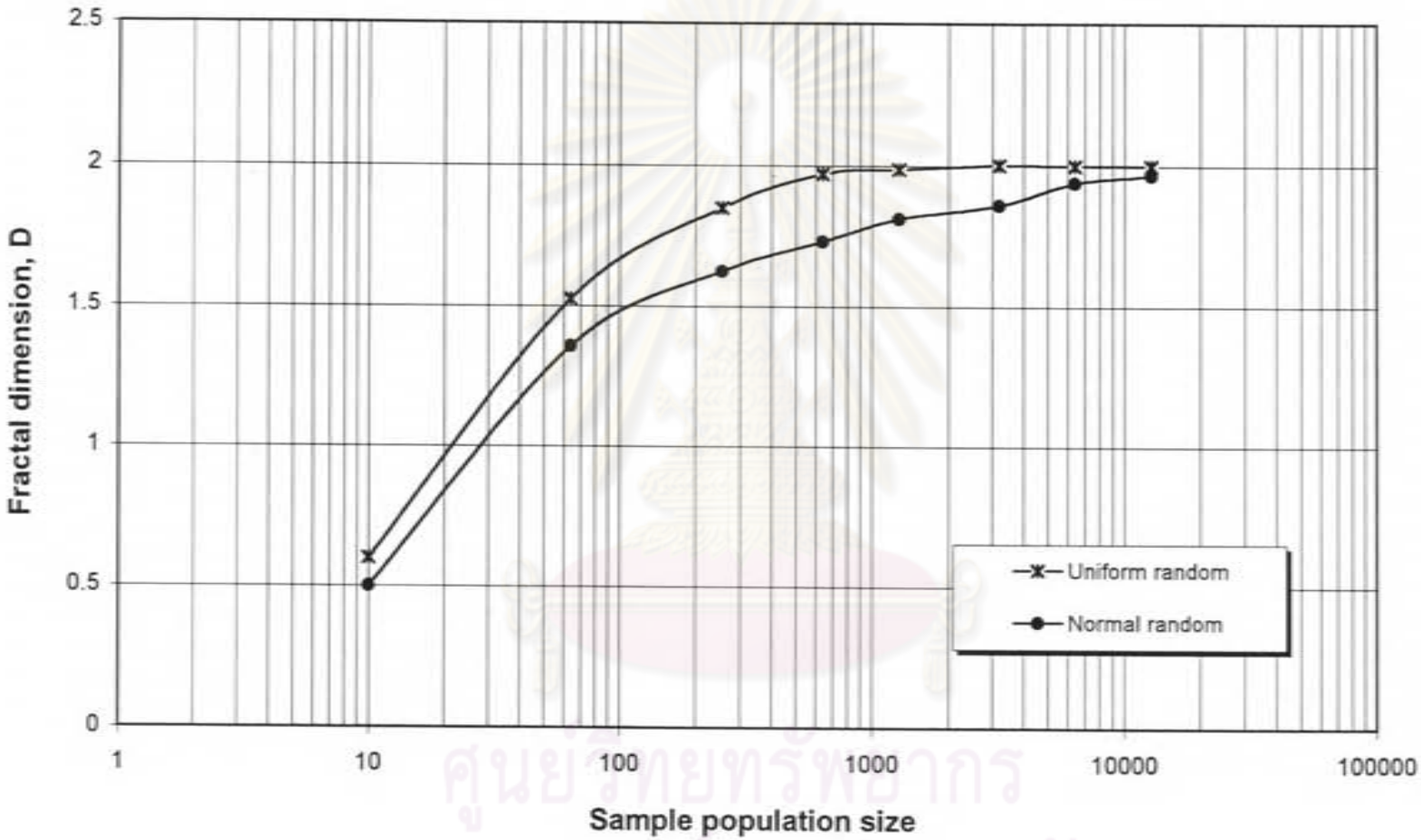

Figure 5.4 Relationship between the observed fractal dimension and the sample population size in the present study (using Eq. (3.4)) for the region of n which provided the maximum slope

Table 5.2 Computer-simulated results (Fractal dimension is found using equation (3.4) for the region of n which provides the maximum slope)

Sample population size	Fractal dimension (D)	
	Uniform random dispersion	Normal random dispersion
10	0.6008	0.5006
64	1.5248	1.3557
256	1.8499	1.6252
640	1.9706	1.7309
1280	1.9875	1.8122
3200	2.0024	1.8607
6400	2.0000	1.9393
12800	2.0000	1.9667

From Figure 5.4, it can be seen that the fractal dimension for both the uniform and normal dispersions increased as the sample population size increased. And the fractal dimension for the uniform random dispersion was always greater than that for the normal random dispersion. Therefore, it can be concluded that a reasonable fractal dimension should be calculated from the region of n which provides the maximum slope. Note that the smaller the sample population size, the smaller the appropriate n to use.

2) Fractal dimension calculated from the coefficient of variation (D_s), (Terashita's approach).

Similarly, the relationship between the sample population size and Terashita's fractal dimension is shown in Figure 5.5 and listed in Table 5.3.

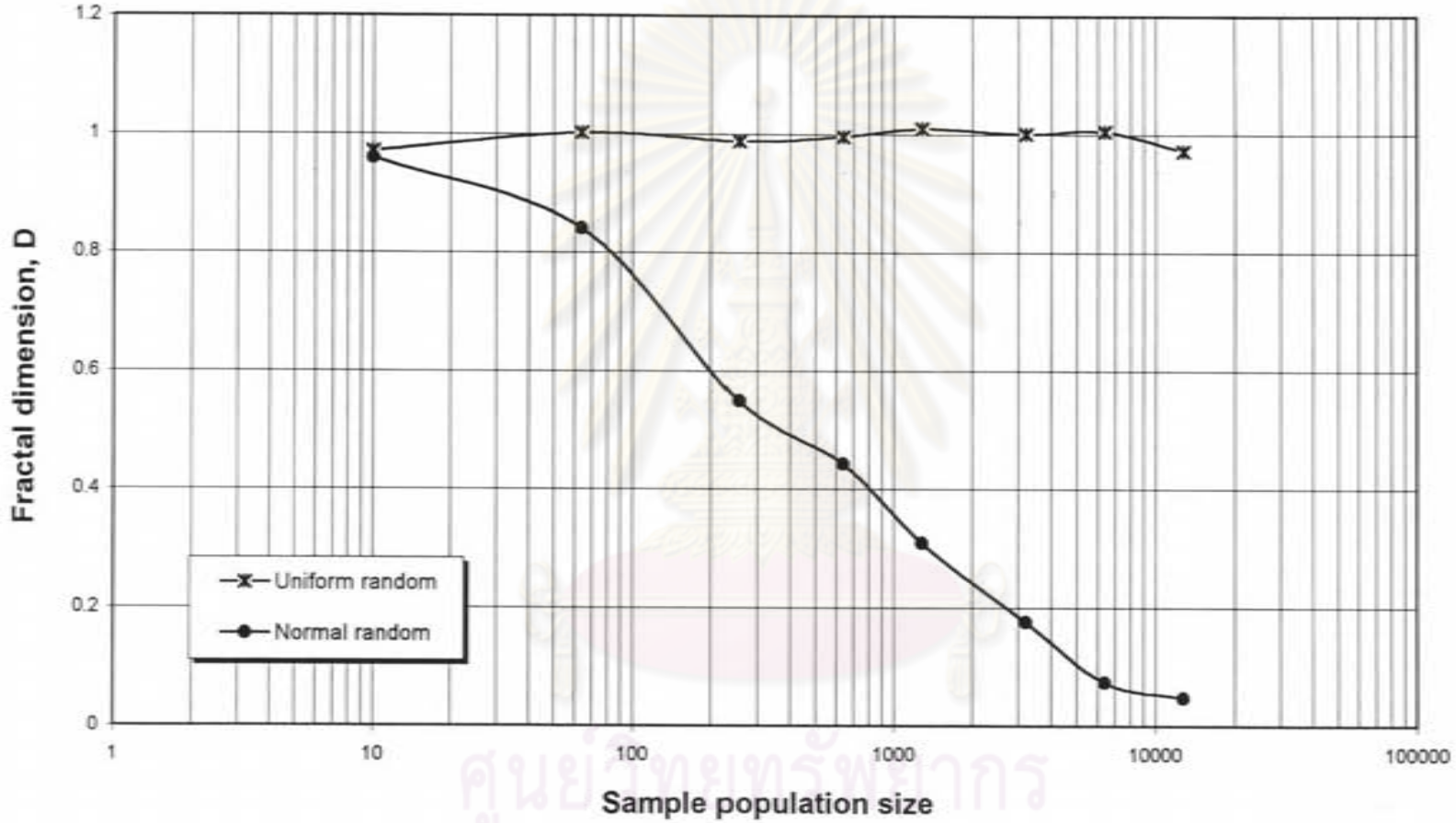

Figure 5.5 Relationship between the observed fractal dimension in Terashita's approach and the sample population size

From Figure 5.5, it can be seen that the observed Terashita's fractal dimension for the uniform random dispersion remained essentially constant around 1, while that for the normal random dimension depended remarkably on the sample population size. Obviously, when only a small number of particles are present in a sample (small sample population size), it is harder to distinguish between good and bad dispersions than when the sample population is large.

Table 5.3 Computer-simulated results (Terashita's fractal dimension)

Sample population size	Fractal dimension (D)	
	Uniform random dispersion	Normal random dispersion
10	0.9707	0.9594
64	1.0022	0.8399
256	0.9872	0.5485
640	0.9955	0.4433
1280	1.0099	0.3091
3200	1.0005	0.1764
6400	1.0052	0.0742
12800	0.9711	0.0473

Generally speaking, Terashita's fractal dimension is a more accurate and robust measure of dispersibility than the one calculated using Eq 3.4. In the case of uniform random dispersion, Terashita's fractal dimension remains essentially unity (between 0.97 to 1.0) regardless of the size of particle population. In the case of normal random dispersion, Terashita's fractal dimension dropped rapidly to 0.04 as the sample population size increased. This confirms the common sense that the larger the sample size, the easier the differentiation between the normal random and uniform random dispersions.

5.2 Effects of kneading conditions on the dispersion of pigments in polystyrene

Since the pigment median particle size in this investigation was very small, 0.20 μm for the iron oxide pigment and 0.095 μm for the carbon black pigment, a sufficiently high magnifying power was necessary to see and distinguish between the magnified pigment particles and smudges or even bubbles. It was found that the magnifying power of the scanning electron microscope should be 5,000X and 15,000X in the case of iron oxide pigment and carbon black pigment, respectively. Figure 5.6 shows some examples of the microphotographs of both pigments that were taken by SEM in the present study.

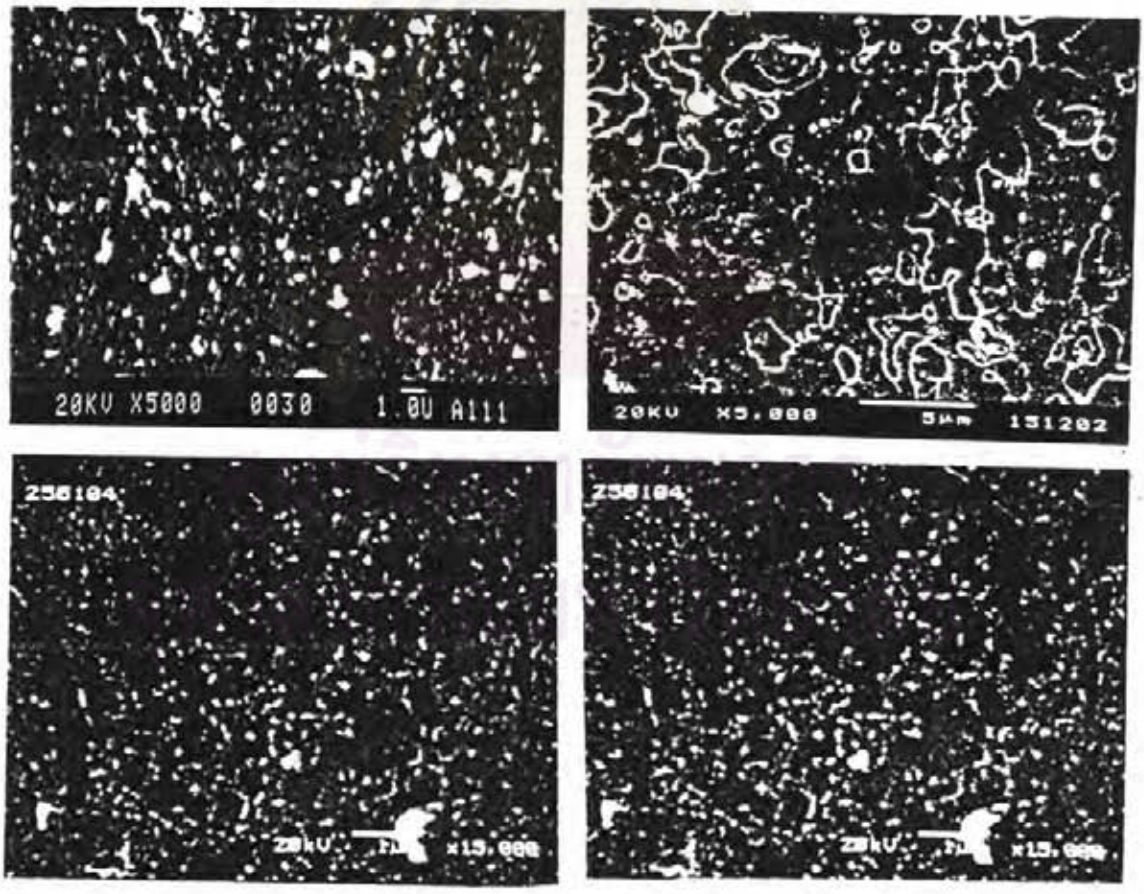

Figure 5.6 Examples of SEM microphotographs

Table 5.4 Effect of kneading conditions on the dispersion of pigment in polystyrene

Kneading temp., T_k, (°C)	Speed of screw, R, (rpm)	Feed rate, F, (g/min)	D (iron oxide)	D (carbon black)
170	81	4.5	1.507	1.697
		22.7	1.528	1.676
		41.4	1.429	1.760
	162	4.5	1.520	1.746
		22.7	1.504	1.750
		41.4	1.465	1.607
	324	4.5	1.650	1.760
		22.7	1.557	1.767
		41.4	1.528	1.721
190	81	4.5	1.519	1.785
		22.7	1.396	1.702
		41.4	1.390	1.617
	162	4.5	1.592	1.845
		22.7	1.553	1.802
		41.4	1.558	1.734
	324	4.5	1.772	1.836
		22.7	1.575	1.804
		41.4	1.527	1.778
210	81	4.5	1.650	1.803
		22.7	1.664	1.780
		41.4	1.330	1.764
	162	4.5	1.740	1.865
		22.7	1.623	1.793
		41.4	1.631	1.790
	324	4.5	1.863	1.869
		22.7	1.758	1.841
		41.4	1.532	1.851

In this study, the effect of kneading conditions on the dispersion of two types of pigments in polystyrene upon using a continuous kneader was investigated. The parameters were kneading temperature, rotational speed of screw, and feed rate. A summary of the experimental results was shown in Table 5.4. The experimental results and discussions may be categorized into three parts as follows:

5.2.1 Kneading temperature

Effect of the kneading temperature on the dispersion of the pigments, iron oxide and carbon black, was investigated at 170, 190, and 210 °C. Figures 5.7 and 5.8 show the effect of the kneading temperature on the dispersion state of iron oxide and carbon black, respectively, which was evaluated using the fractal dimension based on the counting method.

These figures show that, for both the iron oxide pigment and carbon black pigment, the fractal dimension as well as the degree of dispersion tended to increase as the kneading temperature increased. This is because the higher the kneading temperature at which the sample was kneaded, the lower the resulting melt viscosity. In short, the dispersibility of pigment increased as the kneading temperature increased and in this work, the highest kneading temperature (T = 210 °C) shows the highest dispersibility.

5.2.2 Rotational speed of screw

The effect of the rotational speed on the dispersibility of iron oxide pigment and carbon black pigment was investigated at 81, 162, and 324 rpm. The effect of the rotational speed on the dispersion state was depicted in Figures 5.9 and 5.10, respectively.

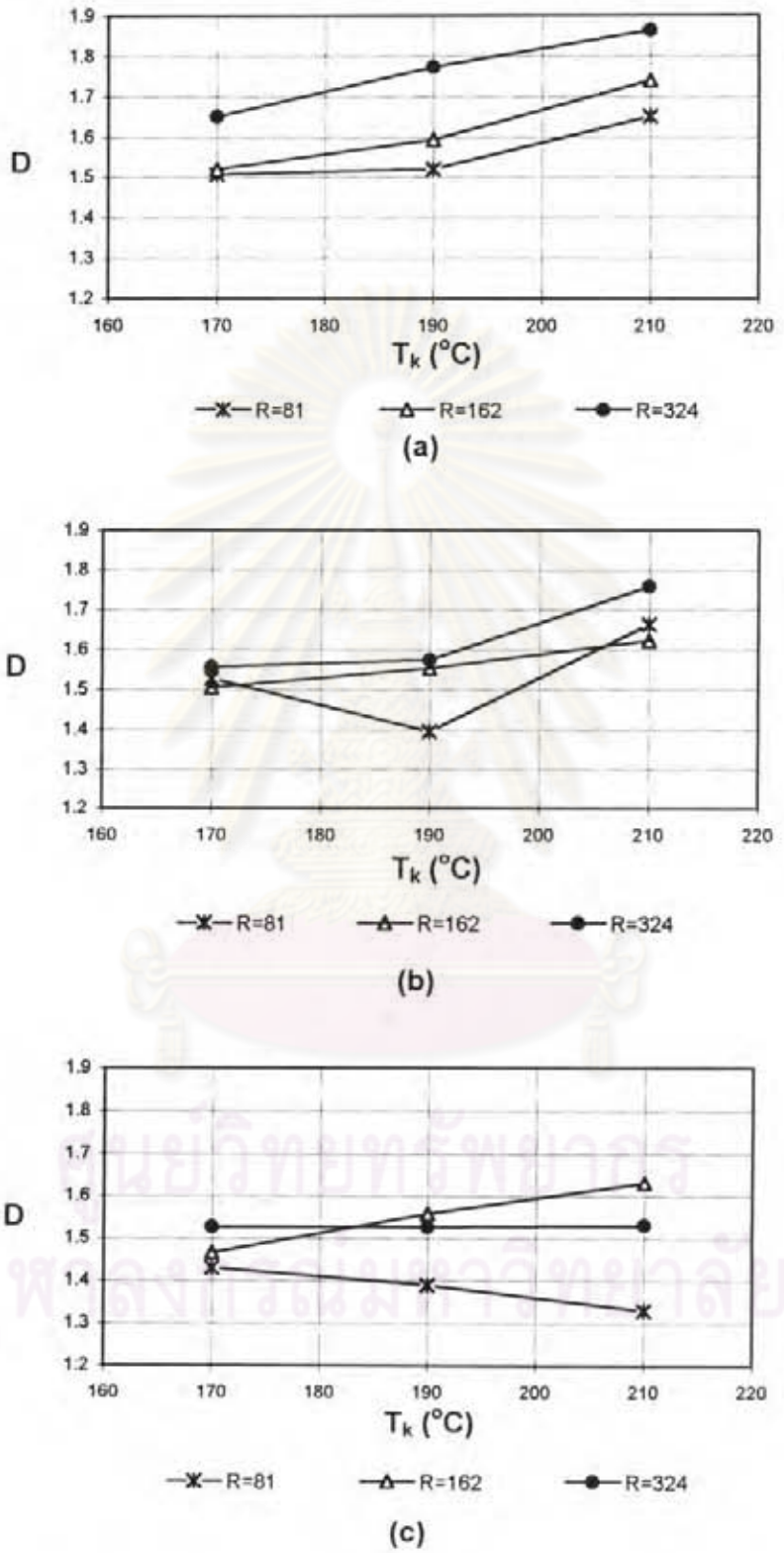

Figure 5.7 Relationship between the kneading temperature (T_k) and the fractal dimension (D) in the case of the iron oxide pigment (a) at F=4.5 g/min; (b) at F=22.7 g/min; (c) at F=41.4 g/min

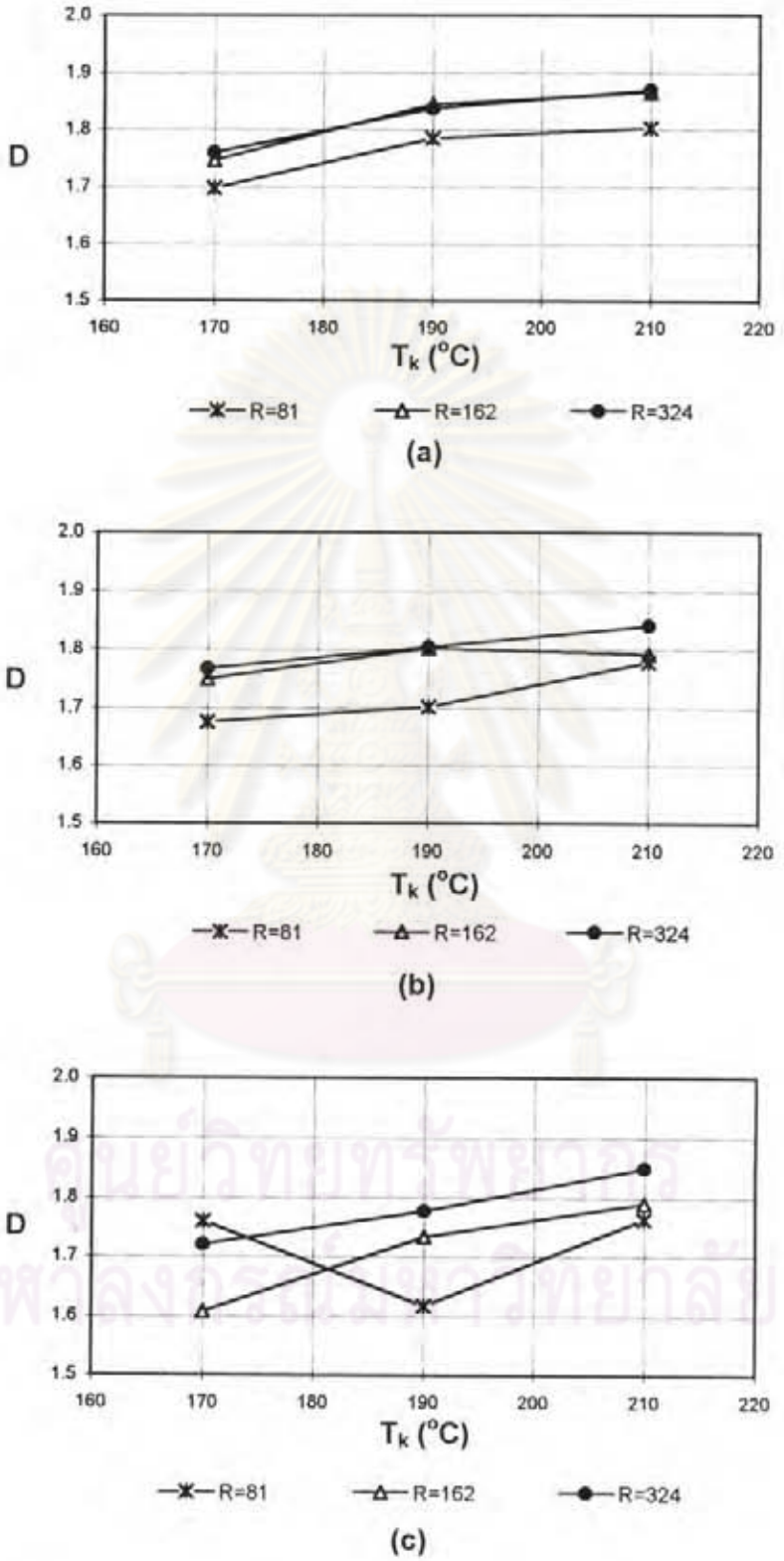

Figure 5.8 Relationship between the kneading temperature (T_k) and the fractal dimension (D) in the case of the carbon black pigment (a) at F=4.5 g/min; (b) at F=22.7 g/min; (c) at F=41.4 g/min

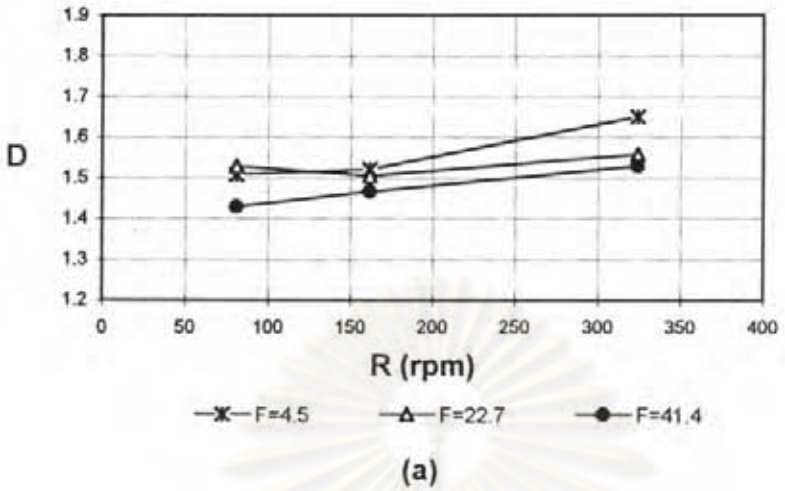

(a)

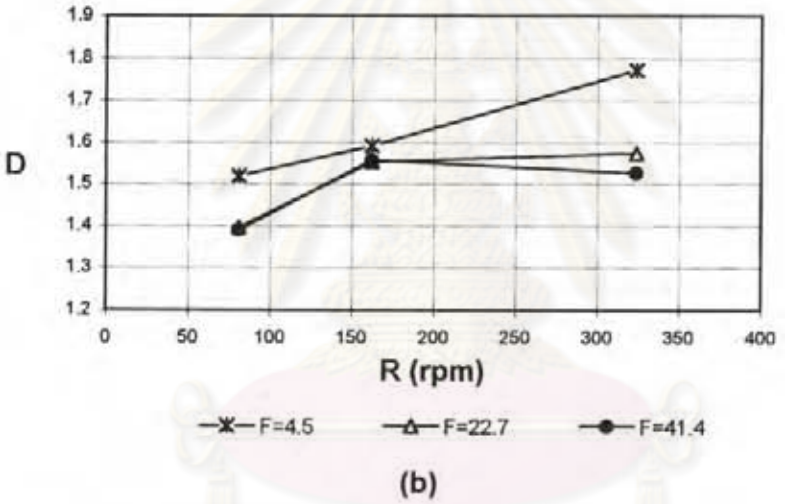

(b)

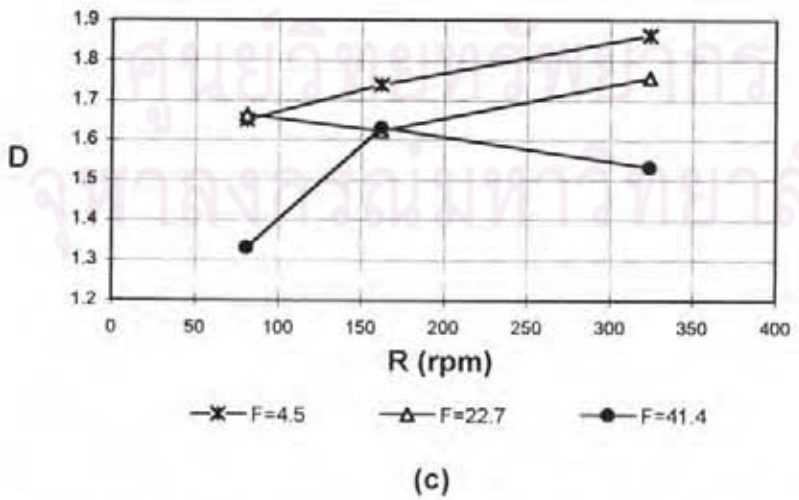

(c)

Figure 5.9 Relationship between the rotational speed of screw (R) and the fractal dimension (D) in the case of the iron oxide pigment (a) at T=170 °C; (b) at T=190 °C; (c) at T=210 °C

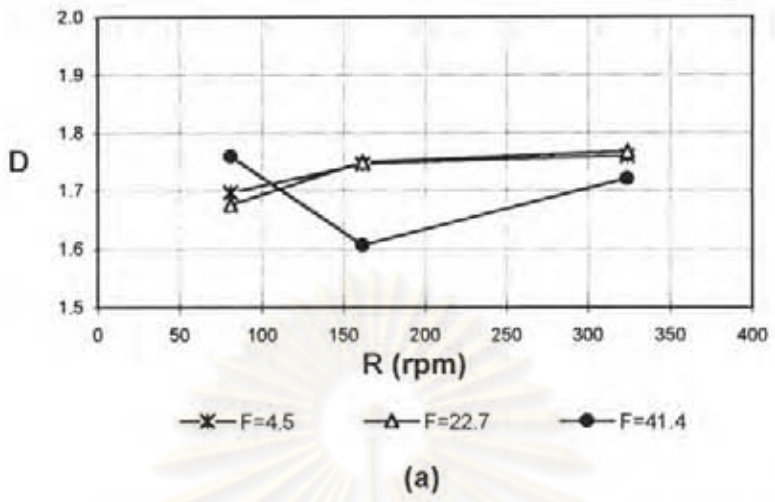

(a)

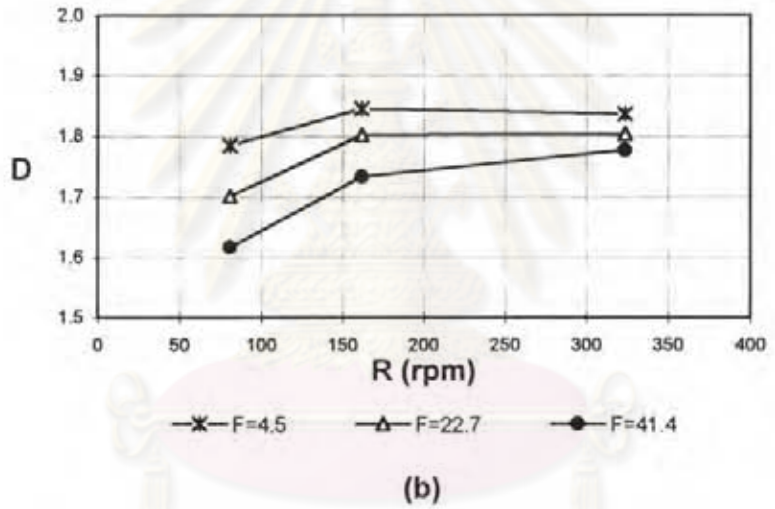

(b)

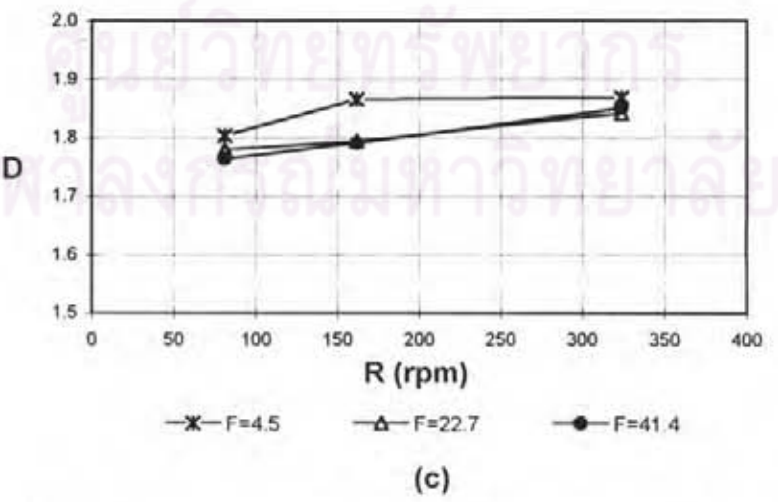

(c)

Figure 5.10 Relationship between the rotational speed of screw (R) and the fractal dimension (D) in the case of carbon black pigment (a) at T=170 °C; (b) at T=190 °C; (c) at T=210 °C

From the above figures, it is obvious that, for both pigments, the fractal dimension tended to increase significantly as the rotational speed increased. This means that as the rotational speed of the screw increased, the dispersion of the pigment particles in the sample was enhanced. The increase in the rotational speed resulted in higher intensity of shear stresses, thus leading to more breakdown of agglomerates and higher degree of dispersion.

5.2.3 Feed rate

The effect of the feed rate of the material to the kneader, which was controlled by the accurate feeder, on the dispersion of pigment was investigated at 4.5, 22.7, and 41.4 g/min. Figures 5.11 and 5.12 show the effect of the feed rate on the dispersion of iron oxide and carbon black, respectively.

These figures show that the fractal dimension tended to decrease as the feed rate increased. This means that as the feed rate increased, the dispersion of pigment in the matrix tended to decrease. At a lower feed rate, the mean residence time was higher. Therefore, the pigment was kneaded into the polymer for a longer time, thus resulting in better dispersion.

5.3 Comparison between pigment types

From the simulation results obtained for the ideal cases, based on both the counting method and Terashita's method, it is obvious that the observed fractal dimension depends significantly on the sample population size. Therefore, because of the unequal numbers of particles in the samples, a straight-forward comparison between the cases of the carbon black pigment and the iron oxide pigment at the same kneading conditions can not be carried out.

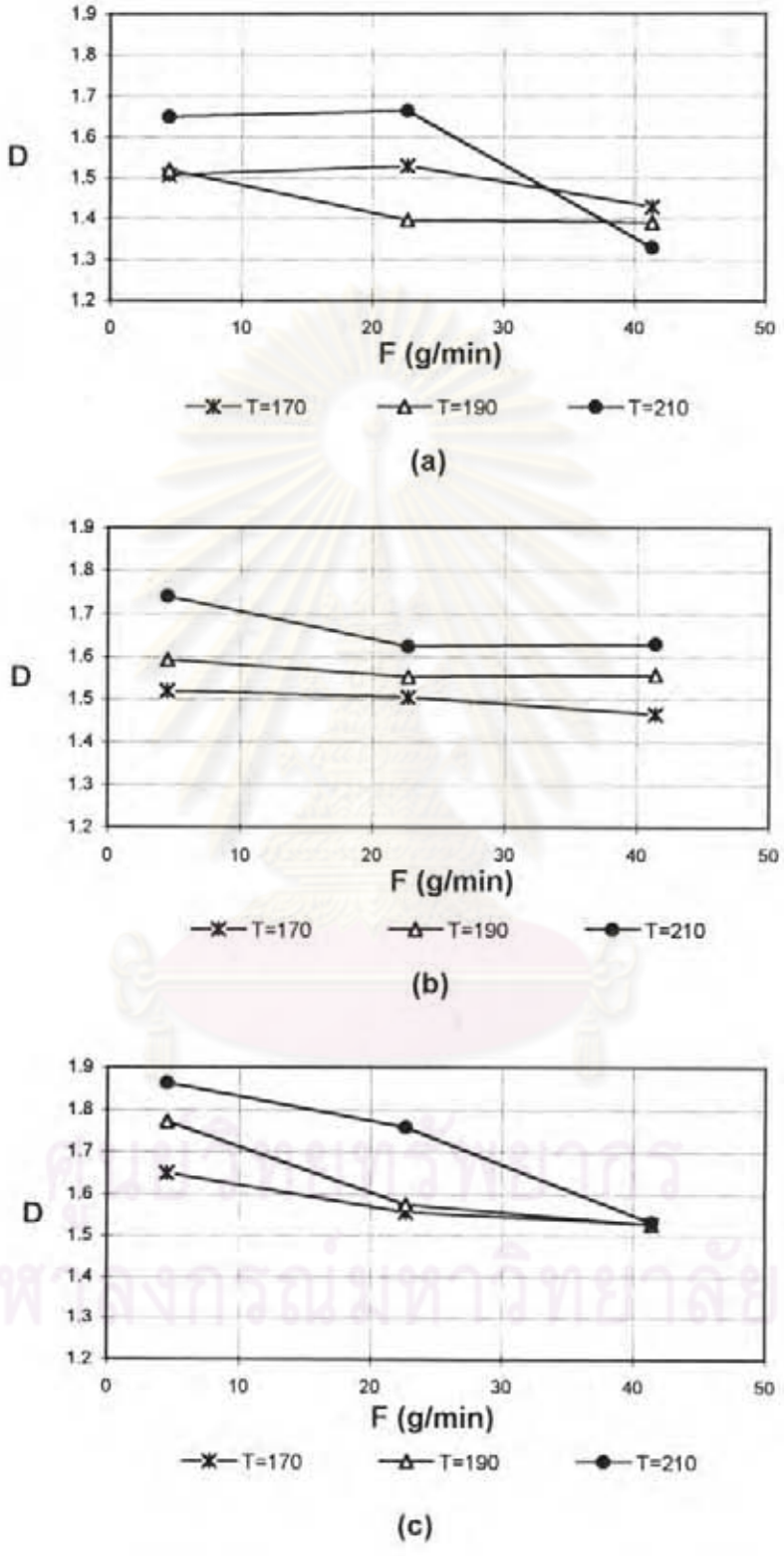

Figure 5.11 Relationship between the feed rate (F) and the fractal dimension (D) in the case of the iron oxide pigment (a) at R=81 rpm; (b) at R=162 rpm; (c) at R=324 rpm

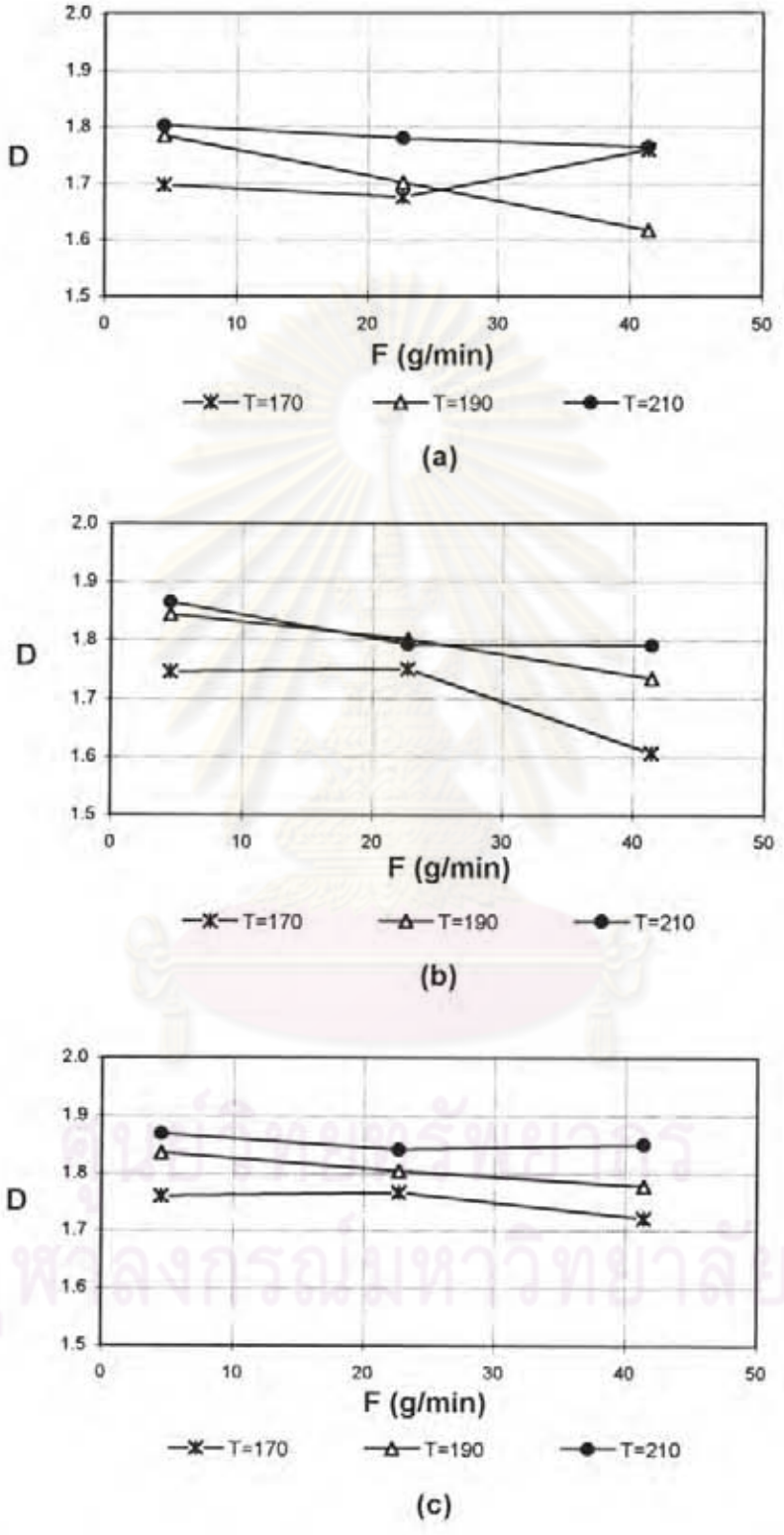

Figure 5.12 Relationship between the feed rate (F) and the fractal dimension (D) in the case of the carbon black pigment (a) at R=81 rpm; (b) at R=162 rpm; (c) at R=324 rpm

The problem can be solved, however, if the experimental result is to be normalized using the corresponding ideal-case value obtained from the computer simulation.

$$D_1^* = \frac{D}{D_{uniform}} \qquad (5.1)$$

where D_1^* = normalized fractal dimension with respect to the uniform random dispersion

D = experimental fractal dimension

$D_{uniform}$ = fractal dimension for the ideal uniform random dispersion with the same sample population size

Similarly it can also be normalized with the respect to the fractal dimension of the ideal normal random dispersion, D_{normal}, in order to evaluate the efficiency of the continuous kneader used.

$$D_2^* = \frac{D}{D_{normal}} \qquad (5.2)$$

where D_2^* = normalized fractal dimension with respect to the normal random dispersion

The experimental results which represented by normalized values of the fractal dimension were shown in Table 5.5.

Table 5.5 Effect of kneading conditions on the dispersion of pigments in polystyrene in terms of normalized fractal dimension

Kneading temp., T_k, (°C)	Speed of screw, R, (rpm)	Feed rate, F, (g/min)	Iron oxide		Carbon black	
			D_1^*	D_2^*	D_1^*	D_2^*
170	81	4.5	0.914	1.026	0.964	1.095
		22.7	0.910	1.033	0.958	1.081
		41.4	0.851	0.959	0.946	1.067
	162	4.5	0.921	1.034	0.981	1.112
		22.7	0.912	1.023	0.967	1.101
		41.4	0.883	0.993	0.940	1.057
	324	4.5	0.959	1.086	0.989	1.121
		22.7	0.907	1.052	0.976	1.111
		41.4	0.909	1.025	0.995	1.147
190	81	4.5	0.949	1.048	0.981	1.109
		22.7	0.900	1.004	0.972	1.098
		41.4	0.869	0.959	0.951	1.078
	162	4.5	0.931	1.055	0.103	1.125
		22.7	0.935	1.049	0.995	1.132
		41.4	0.922	1.039	0.979	1.111
	324	4.5	0.990	1.197	0.993	1.120
		22.7	0.937	1.057	0.986	1.107
		41.4	0.904	1.018	0.971	1.104
210	81	4.5	0.965	1.092	0.996	1.134
		22.7	0.935	1.060	0.989	1.112
		41.4	0.887	0.964	0.975	1.109
	162	4.5	0.986	1.115	1.008	1.137
		22.7	0.941	1.064	0.990	1.128
		41.4	0.932	1.052	0.989	1.126
	324	4.5	1.018	1.193	1.027	1.161
		22.7	0.987	1.120	1.017	1.158
		41.4	0.957	1.057	1.000	1.128

$D_1^* = D/D_{uniform}$

$D_2^* = D/D_{normal}$

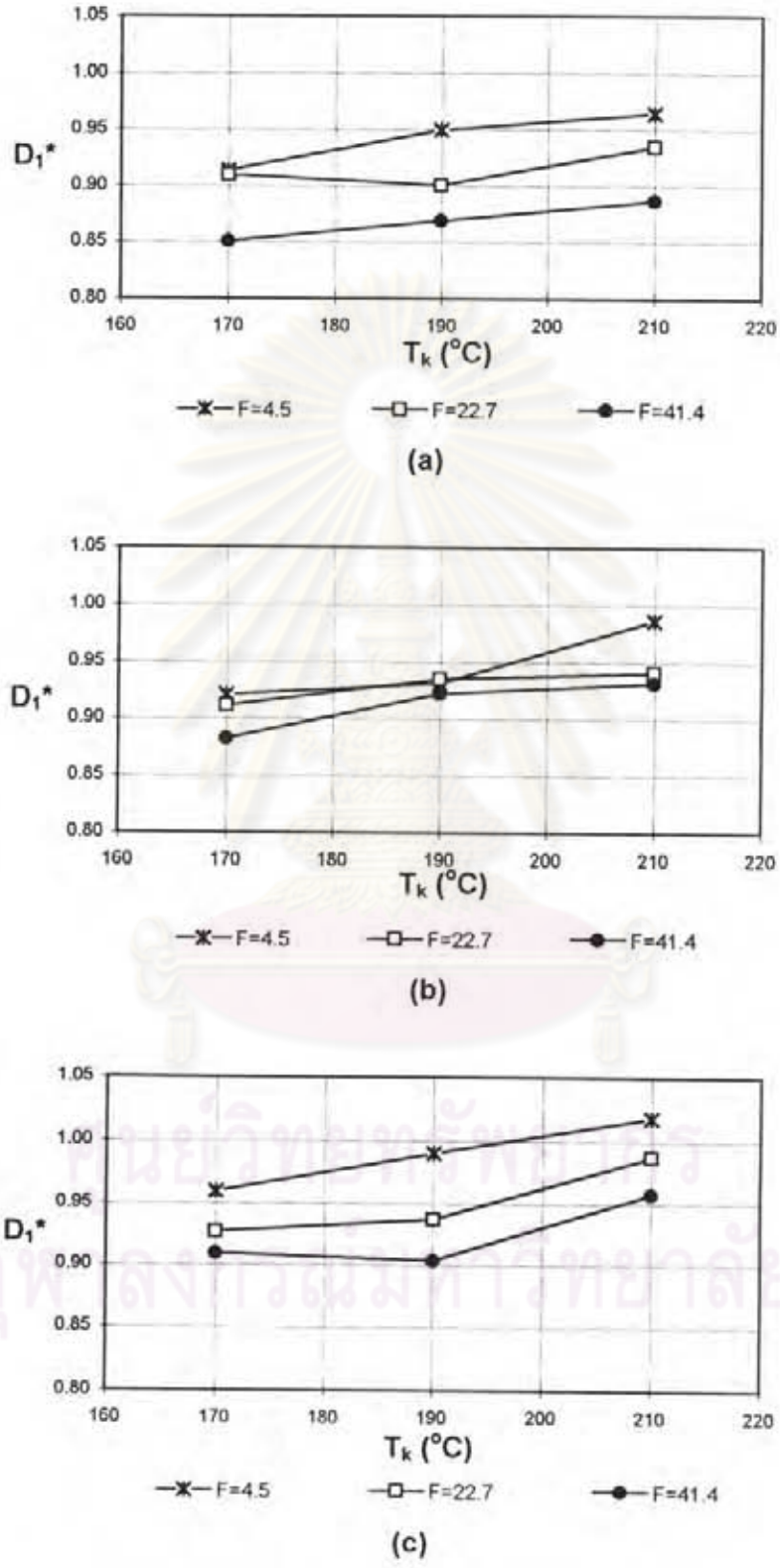

Figure 5.13 Relationship between the kneading temperature (T_k) and the normalized fractal dimension (D_1^*) in the case of the iron oxide pigment (a) at R=81; (b) at R=162; (c) at R=324

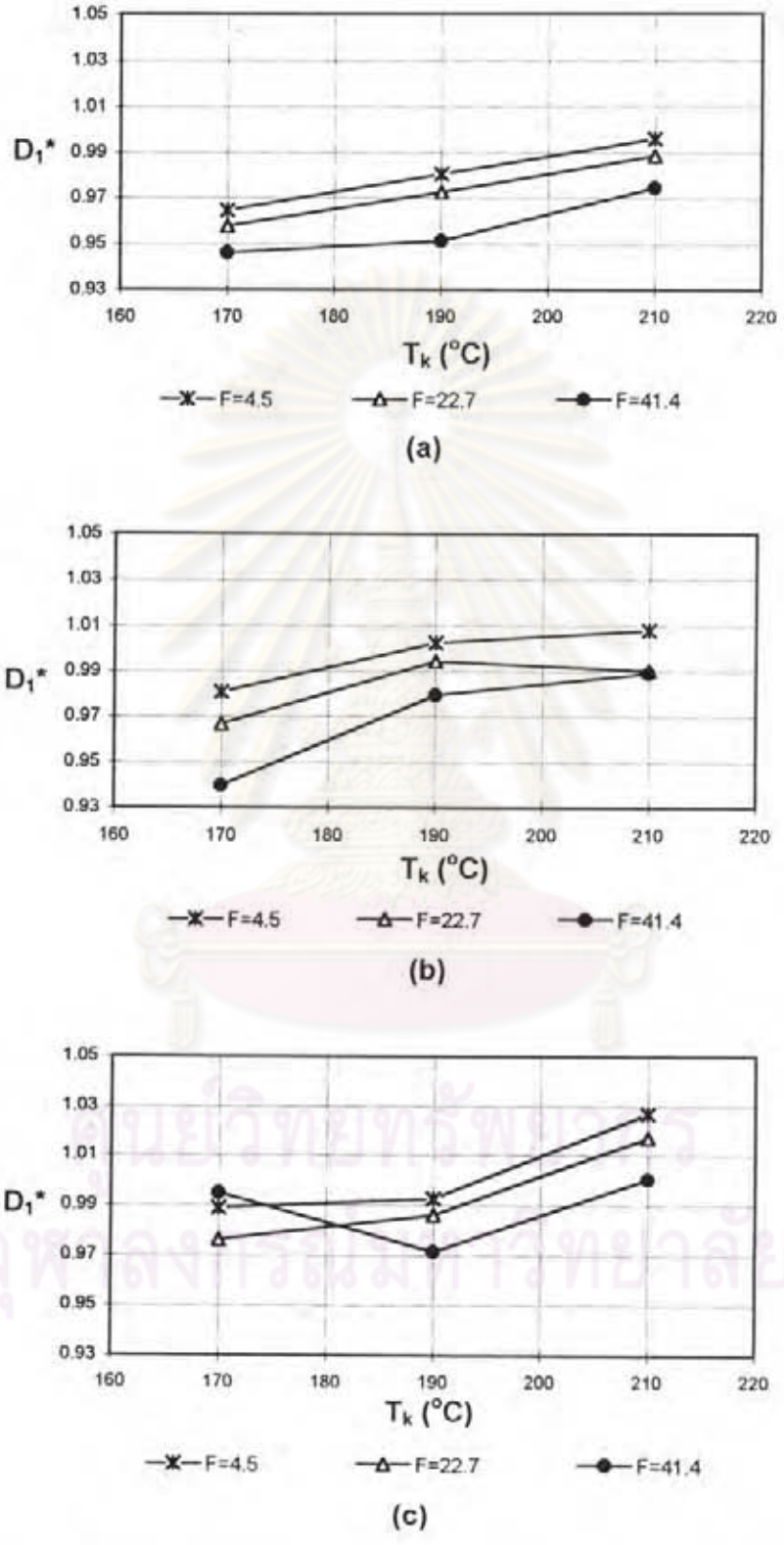

Figure 5.14 Relationship between the kneading temperatureand the normalized fractal dimension (D_1^*) in the case of carbon black pigment (a) at R=81; (b) at R=162; (c) at R=324

5.3.1 Kneading temperature

Figures 5.13 and 5.14 show the effect of kneading temperature on the dispersion state of iron oxide and carbon black, respectively. It can be seen that the normalized values of the fractal dimension in the case of the carbon black were greater. This means the carbon black pigment dispersed more uniformly than iron oxide pigment. This may be because the physicochemical properties of carbon black is more compatible with polystyrene than those of iron oxide.

5.3.2 Rotational speed of screw

Comparison between Figures 5.15 and 5.16 reveals that the normalized values of the fractal dimension in the case of the carbon black was greater. This is because the particle size of carbon black pigment was smaller, carbon black being 0.095 μm and iron oxide 0.20 μm, and absorbed moisture was greater. Therefore, it has higher tendency to agglomerate. From the theoretical discussion on dispersion mixing (Ahmed, 1979), larger agglomerates would disperse more easily than the smaller ones. This explains why that the carbon black pigment dispersed more uniformly than iron oxide pigment.

5.3.3 Feed rate

Comparison between Figures 5.17 and 5.18 shows that the carbon black pigment was dispersed more uniformly than iron oxide pigment. This may be because of pigment properties as mentioned in 5.3.1.

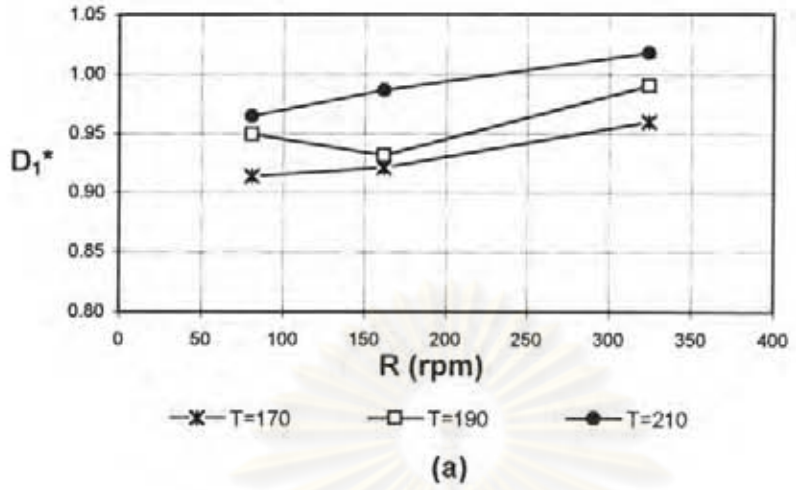

(a)

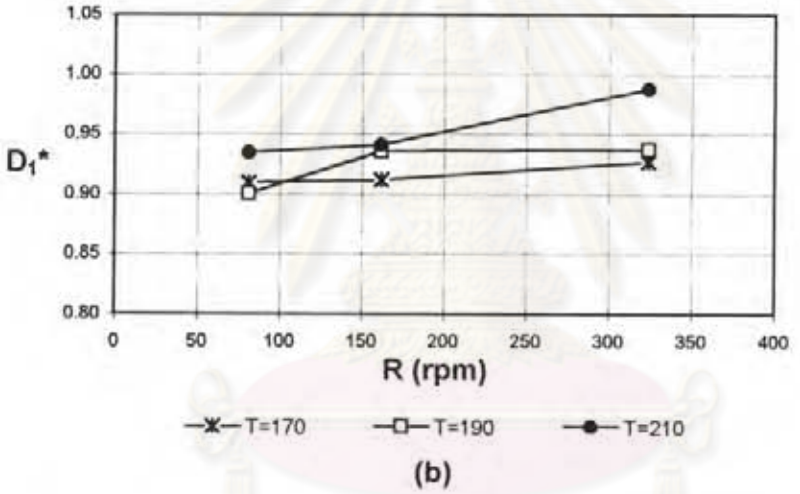

(b)

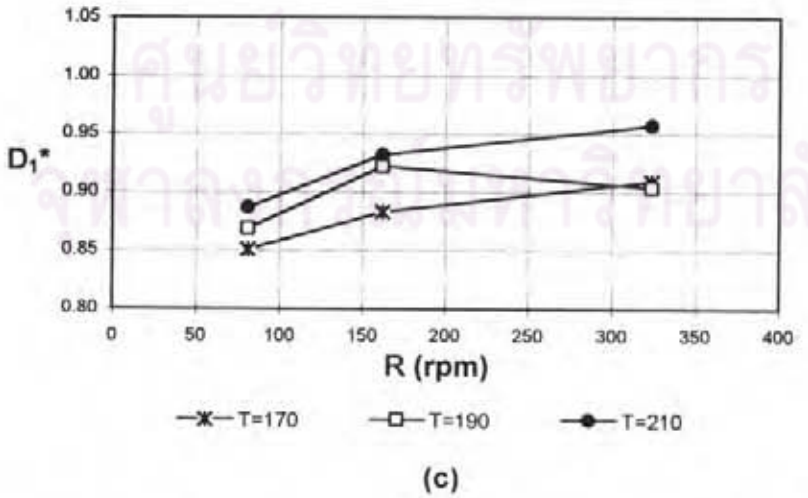

(c)

Figure 5.15 Relationship between the rotational speed of screw (R) and the normalized fractal dimension (D_1^*) in the case of the iron oxide pigment (a) at F=4.5 g/min; (b) at F=22.7 g/min; (c) at F=41.4 g/min

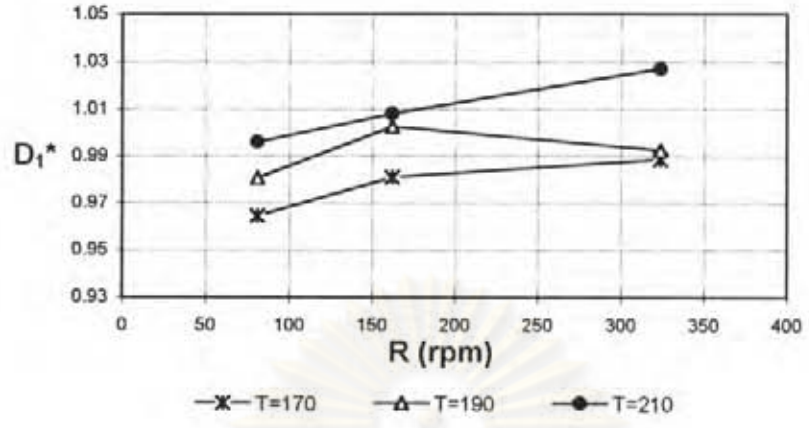

(a)

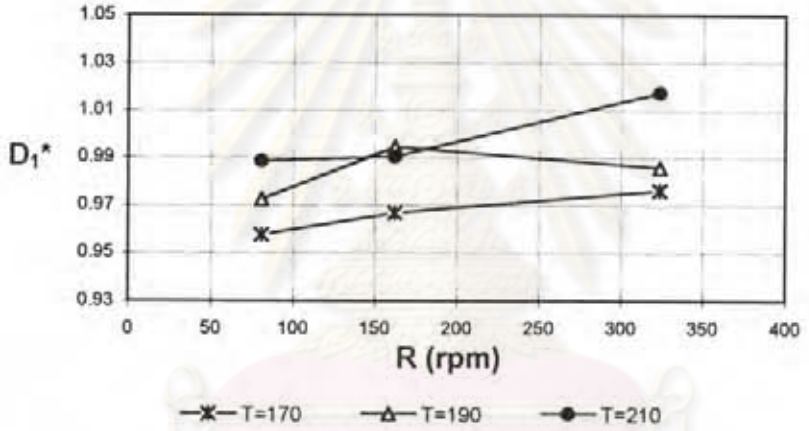

(b)

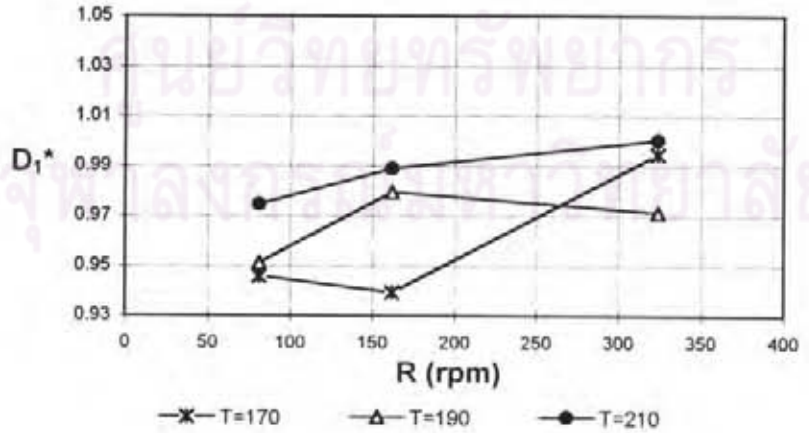

(c)

Figure 5.16 Relationship between the rotational speed of screw (R) and the fractal normalized dimension (D_1^*) in the case of carbon black pigment (a) at F=4.5 g/min; (b) at F=22.7 g/min; (c) at F=41.4 g/min

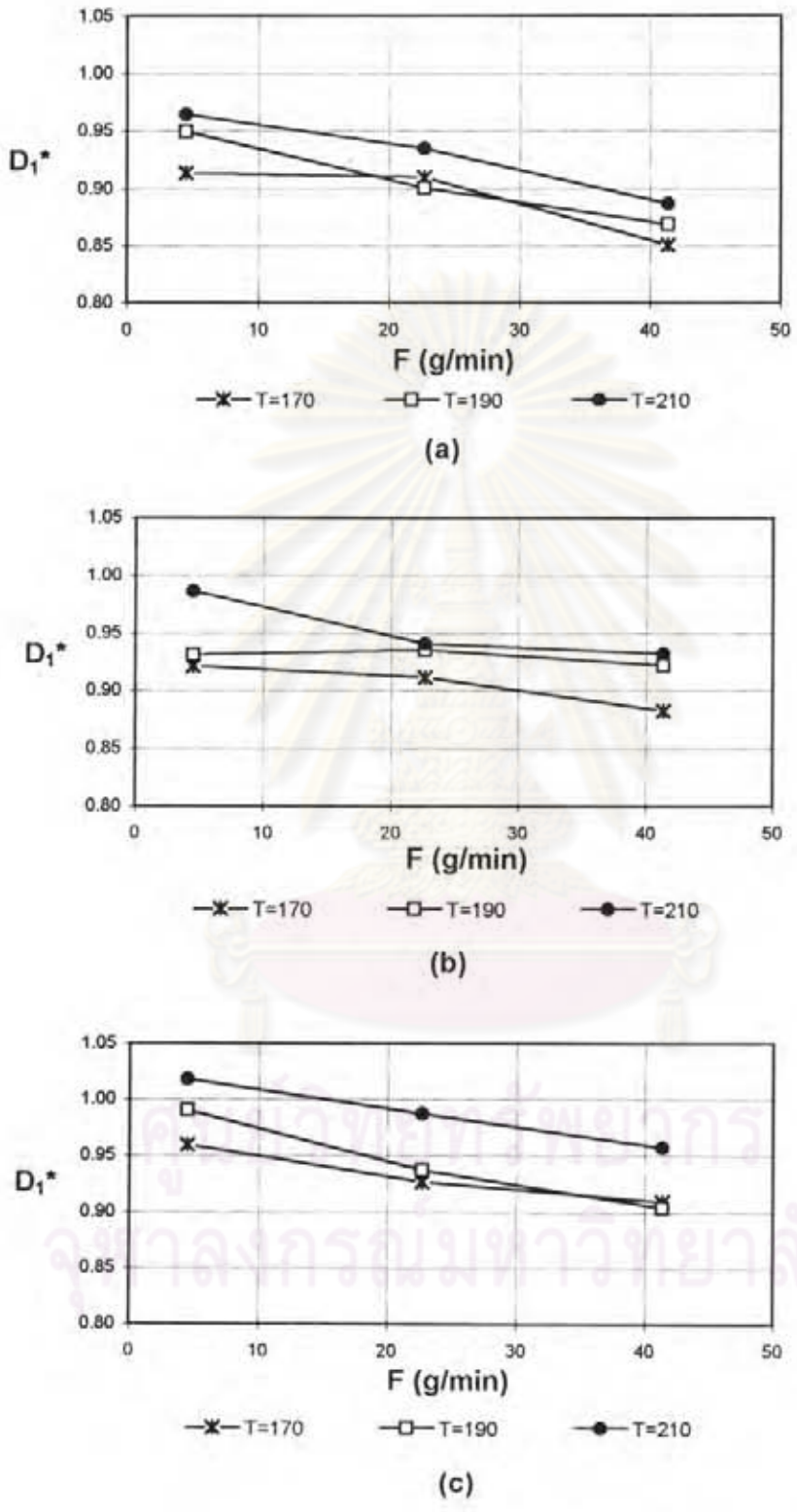

Figure 5.17 Relationship between the feed rate (F) and the normalized fractal dimension (D_1^*) in the case of the iron oxide pigment (a) at R=81 rpm; (b) at R=162 rpm; (c) at R=324 rpm

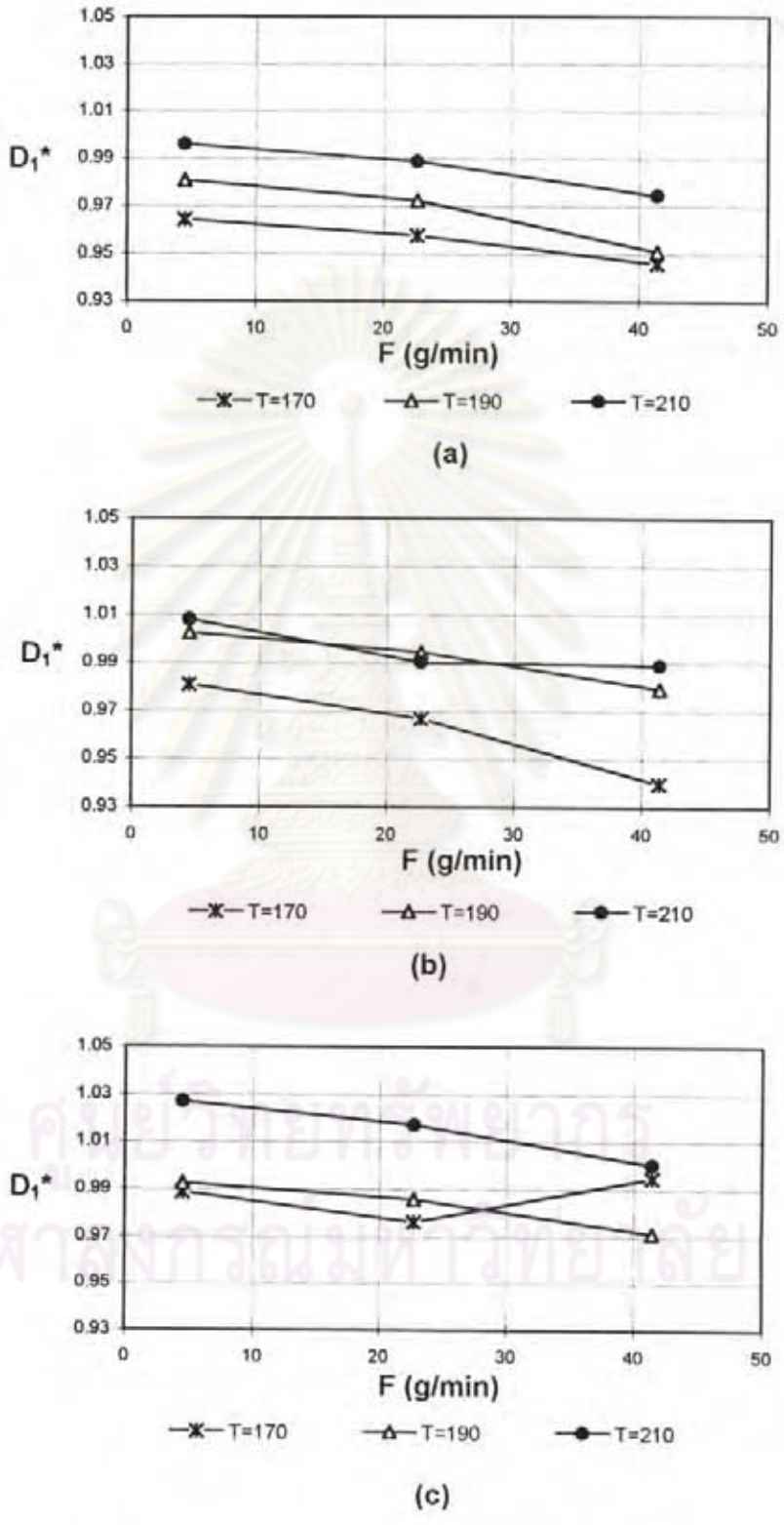

Figure 5.18 Relationship between the feed rate (F) and the normalized fractal dimension (D_1^*) in the case of carbon black pigment (a) at R=81 rpm; (b) at R=162 rpm; (c) at R=324 rpm

From the above sections 5.2 and 5.3, the experimental results for both the iron oxide pigment and carbon black pigment, it may be concluded that at a higher kneading temperature dispersibility of the pigment in the polymer was enhanced. Regarding the rotational speed of the twin screws, a higher rotational speed yielded higher dispersion because it raised the intensity of energy input and led to an increased level of shear stresses transmitted through the kneaded material. The highest rotational speed of 324 rpm. was the most suitable. And when feed rate was low, the retention time in the kneader was long, so the dispersibility was enhanced.

It can be seen that, for both of the pigments, the effects of the kneading conditions showed the same trends. However, the observed values of the fractal dimension in the case of carbon black were greater because the numbers of particles in the samples that were analyzed were greater, which corresponded the simulated ideal-case results. Even when the experimental values of the fractal dimension were normalized with the corresponding ideal values obtained from simulation, it was found that the normalized values of the fractal dimension in the case of the carbon black were still greater. This may be because the physicochemical properties of carbon black is more compatible to polystyrene than those of iron oxide.

5.4 Dispersion efficiency of present kneader

The fractal dimension obtained experimentally and by ideal-case computer simulation are compared here and a summary of the comparison was also shown in Table 5.5.

From the table, it was found that , for both pigments, the values of D_1^*, which were obtained by normalizing the experimental result with the corresponding ideal-case values with respect to the uniform random dispersion are slightly smaller than 1. On the other hand, almost all values of D_2^* which where normalized with the corresponding ideal-case values with respect to the normal random dispersion are greater than 1, in some cases nearly 1.2. This means the continuous kneading used in the present study provided the kneaded material with dispersibility of pigments not truly uniform but a few and up to 20% better than in the case of the normal random dispersion. The normalized values of the fractal dimension (D_1^* and D_2^*) in the case of carbon black pigment were generally greater than in the case of iron oxide pigment, which confirms our conclusion that carbon black dispersibility is better than iron oxide.